

The Effect of Dolphin Echolocation-Fuzzy Logic Controller in Semi-active control of structural systems by using endurance time method

Farzam Moghadam-Rad ^a, Panam Zarfam ^{a,*} and Masoud Zabihi-Samani ^b

^a *Department of Civil Engineering, Science and Research Branch, Islamic Azad University, Tehran, Iran.*

^b *Department of Civil Engineering, Parand Branch, Islamic Azad University, Tehran, Iran.*

Abstract. An adaptive fuzzy-logic -controller (FLC) is proposed to actuate MR damper smartly. Minimizing the excessive responses of building should be considered as a multi-objective optimization problem. The new generation structural systems should be designed based on seismic performance level. Designing based on performance requires dynamic, heavy and repetitive time history analyses. The endurance time analysis method (ETA) is a modern dynamic method based on the performance of the structure, which leads to the reduction of time and number of structural analyses. To investigate the efficiency of Dolphin Echolocation-Fuzzy Logic Controller (DE-FLC) and ETA, several ET simulations were performed. The seismic responses of 11th-story benchmark building equipped with MR dampers were investigated in two cases of seven time-history analysis and six generation of ET functions. By using Dolphin echolocation, the optimal arrangement and the number of sensors and dampers is determined. The proposed DE-FLC controller demonstrates its efficiency by reducing the excessive displacement under seismic excitations in comparison with uncontrolled case and classical FLC. Furthermore, the results demonstrate that sixth generation of ETA can simulate responses of several time-history analyzes well with proper accuracy, without necessitating any several computational burden.

Keywords: Semi-active control of smart buildings, Fuzzy logic control, Dolphin echolocation (DE), Magnetorheological damper, Endurance time analysis (ETA).

* Corresponding author. E-mail: zarfam@sbiau.ac.ir

E-mail mzabihi@iust.ac.ir (Masoud Zabihi-Samani); farzammr@yahoo.com (Farzam Moghadam-Rad)

1. Introduction

To ensure the life usability and reliability in purposing of structural systems, the dissipation of excessive vibration from natural hazards is crucial. Control systems have been utilized as one of the most promising technologies in structural design. A modern controller could have been utilized in new generation buildings to diminish the undesired responses [1]. A passive, semi-active, active and hybrid control devices have been introduced and utilized [2]. Performance of passive control devices are admissible, however the lack of compatibility with undesirable vibration condition was the most problems in robustness and efficiency of the building with this equipment. Active control devices have been introduced and designed, but it requires more developing to dissolve the energy consumption during excitations and robustness obstacles[3].

By emerging smart fluids, the semi-active devices have been utilized in the buildings. A semi-active control system does not use any external force into the structural system. Several studies have been accomplished to develop proprietary control algorithms which could enhance the unique characteristics of MR Fluids [4]. In smart structural systems, MR dampers are new semi-active control devices, which could enhance the vibration control technology [5]. MR dampers have the reliability of passive control devices concurrent with the versatility and adaptability of active control devices. It contains a semi-fluid in the piston, which could change the "shock" energy into heat by transferring the fluids between two different chambers via tiny orifices. By transmitting the electrical current, a coil inside the piston constructs a magnetic field and modifies the characteristics of the MR Fluid. Therefore, the resistance of the damper can be continuously modified online by modulating electrical current to the damper fluids, instantaneously. Large scale MR dampers have been fabricated and several full-scale structures have been utilized semi-active devices to reduce the undesirable vibration responses[6-8].

To formulate the mechanical behavior of MR dampers, Bouc–Wen hysteresis model has been proposed [9]. The application of MR damper in structural systems is more progressive and the economical parameters should be considered in an optimized controller. Different control levels could be utilized by changing arrangement of dampers. Hence, optimal damper arrangement should be accomplished. Furthermore, it is important to reduce the cost of purchase, installation, operation and maintenance of the semi-active devices [10]. Several researches have been investigated on optimal arrangement of dampers [11] but optimal MR damper arrangement and their sensors as two discrete subjects have not paid attention yet [12-14].

Classical optimization methods are not compatible for solving complex engineering problems. The recent generation of the optimization algorithms is meta-heuristics, which are suggested to solve multi-objective engineering problems. A Meta-heuristic algorithm consists of a group of search agents which research the possible region based on both randomization and some predefined rules[15]. These optimization algorithms inspired from natural behavior of animals in nature such as dolphins, etc. The dolphins transmit two intertwined ultrasound beams at different frequencies at different times during the process of echolocation. Scientist developed a mathematical formulation to successfully extricated and read the overlapping signals. This discovery could inspire sharper image quality on ultrasound technology [16]. The computational time of control system should be minimized to eliminate the time delay effects. The Dolphin Echolocation algorithm demonstrated the fast and reliable optimization in comparison with other algorithms, such as genetic algorithm, particle swarm optimization, ant colony optimization in several researches[17-20]. The dolphin echolocation optimization algorithm was proposed based on the process of foraging preys utilizing echolocation in dolphins, which was familiar to discovering the optimal solution on a search space. Kaveh and Farhodi idealized the dolphin echolocation to optimization algorithm [21].

Among the several structural controllers have been provided so far, the Fuzzy logic controller (FLC) have provided the stable, reliable and appropriate semi-active control results in reducing the response of structures during sever earthquakes[22, 23]. However, classical controllers require some pre-known and exact information about the specifications of a structural system that its mathematical matrix is going to be prepared. Furthermore, complex controller such as Linear Quadratic Gaussian (LQG) requires a solution for comprehensive constrained multi-objective optimization problems [24]. As a result, soft-computing techniques have been proposed to attenuate the complexity of those obstacles, such as neural networks[25] and fuzzy logic[26]. Thereupon, recent studies pursued adaptive controllers because they are more reliable and effective[27, 28]. In this research, a Dolphin Echolocation-Fuzzy Logic Controller was proposed to combine the positive aspects of both methods.

To investigate the performance of structures during seismic motions, several analytical methods have been proposed, including static linear, linear dynamic dynamics, nonlinear static and nonlinear dynamic methods. However, due to the shortcomings and limitations of static methods, this method cannot be used in functional analysis. On the other hand, although dynamic methods have a better suitability but they are very time consuming and costly due to the high number of analyzes. As a consequence, to improve the shortcomings of the previous seismic analysis methods, a new incremental dynamic method called the Time Endurance Analysis(ETA) is proposed[29]. By applying a

series of pre-designed accelerator increment functions, the seismic performance of the structure is examined. ETA provides an appropriate estimation of the structure's response to the intensity of different excitations based on the ASCE design spectrum. In comparison with other methods, this method reduces the number of required analyzes to evaluate the structure, without necessitating heavily computational burden. Furthermore, ETA compared to other linear and nonlinear had not any restrictions on considering the behavioral complexities of the structure such as non-linear behavior, effect of control systems, etc. The ETA method is demonstrated the appropriate efficiency in analyzing of structures equipped with passive damper[30, 31]. According to the author's best knowledge, any researches have not been investigated about efficiency of ETA in the structural systems equipped with semi active dampers, yet.

Based on the heavily computational burden, which is required in several seismic time history analyses. In this research, the utilization of ETA analysis is proposed to reduce the time and number of computational analysis requirement in designing of semi-active controller system. Furthermore, a Dolphin Echolocation-Fuzzy Logic Controller (DE-FLC) are proposed to utilize the adoptability of fuzzy logic controller simultaneous with the speed of Dolphin echolocation optimization algorithm. An effective DE-FLC is utilized to enhance the MR damper proficiency and less external energy consumption during seismic excitation. DE-FLC administers the MR damper output force by transmitting electrical input current. To identify the absolute velocity and the displacement of stories independently, separate sensors were determined. For this purpose, the DE-FLC calculates inducing electrical current to produce the magnetic field based on the displacement and the velocity of the floors. The excessive responses of 11th-story building equipped with MR dampers were investigated in two case of seven time-history analysis and six generation of ET functions. Simultaneously, the optimal arrangement and the number of sensors and dampers is determined by Dolphin echolocation. The proposed DE-FLC controller demonstrates its efficiency by reducing the excessive displacement under earthquake in comparison with uncontrolled case and classical FLC. The results demonstrate that sixth generation of ETA can simulate the results of several time history analyzes well, without necessitating any several computational burden.

2. The MR Damper model description and simulation assumptions

The principal subject in planning of semi-active structural controller is which semi-active control strategy should be used. The time-delay effect leads to attenuating the reliability of structural controller. A semi-active controller, which reduces the analysis processing time and does not need any modification during the natural hazards, will have more proficiency. FLC gathers these characteristics to the structural controller. By transmitting external voltage supply, the DE-FLC administrates the MR dampers mechanical behavior. To enhance the efficiency of controller, location of sensors was determined independent from dampers arrangement. Moreover, to determine the external forces of damper, the input data of FLC were defined to absolute velocity and displacement of stories. Furthermore, more stories were involved to determining the damper forces. The semi-active controller should be optimized to minimize the control force of dampers and structural vibration magnitudes. For this purpose, the multi-objective optimization problem, which consists of three objective functions to be optimized. The arrangement of sensors and dampers are considered as search space of optimization process. For optimal arrangement problem, the number of utilized sensors and MR dampers were considered as optimization constraints. The DE-FLC is utilized to solve the MR damper and sensor optimization problem. A state space should be utilized to simulate the displacement and velocity of MR damper over a wide range of loading situations. MR Dampers consists of a semi-solid fluid, which transfers between two different chambers. A coil generates a magnetic field and modifies the characteristics of the MR Fluid in the piston when electrical current is applied. The ability of MR fluids to modify from free-flowing viscous fluids to semi-solids fluids in MR damper was utilized. Therefore, in a few milliseconds, MR damper has an adjustable control force when subjected to a magnetic field. Magneto-rheological fluid has ability to respond to applied magnetic field with a rapid modification by maintaining reversibility of properties. Since 1996, 20 Ton MR dampers have been experimentally tested, designed and utilized [24]. The equations of n-story structure responses could be defined by the following equation:

$$\dot{y}(t) = C.Z(t) + D.u(t) \quad \dot{Z}(t) = A.Z(t) + B.u(t) \quad (1)$$

Where:

$$\begin{aligned}
 A &= \begin{bmatrix} 0_{n \times n} & I_{n \times n} \\ -M_S^{-1} \cdot K_S & -M_S^{-1} \cdot C_d \end{bmatrix} & B &= \begin{bmatrix} 0_{n \times n} & 0_{n \times n} \\ -I_{n \times n} & -M_S^{-1} \cdot D_p \end{bmatrix} \\
 C &= \begin{bmatrix} I_{n \times n} & 0_{n \times n} \\ 0_{n \times n} & I_{n \times n} \\ -M_S^{-1} \cdot K_S & -M_S^{-1} \cdot C_d \end{bmatrix} & D &= \begin{bmatrix} 0_{n \times n} & 0_{n \times n} \\ 0_{n \times n} & 0_{n \times n} \\ -I_{n \times n} & -M_S^{-1} \cdot D_p \end{bmatrix} \\
 Z(t) &= \begin{bmatrix} X_{n \times 1} \\ \dot{X}_{n \times 1} \\ \ddot{X}_{n \times 1} \end{bmatrix} & u(t) &= \begin{bmatrix} \ddot{X}_{n \times 1} \\ F(t)_{n \times 1} \end{bmatrix} & y(t) &= \begin{bmatrix} X_{n \times 1} \\ \dot{X}_{n \times 1} \\ \ddot{X}_{n \times 1} \end{bmatrix}
 \end{aligned} \tag{2}$$

\ddot{x} , \dot{x} and x , in equation (2), are acceleration, velocity and displacement vectors, respectively. The mass, stiffness and damping matrices are represented by M_S , K_S and C_d , respectively. $u(t)$ is output vector of the state space and $F(t)$ is the force of damper. D_p , $Z(t)$ and $y(t)$ demonstrate the damper placement, the state-space and output vector, respectively. In a close-loop process, the DE-FLC determines the control force of MR damper, as a function of velocity and displacement responses of the building. Determining the optimal position and number of dampers and sensors is one of the main economic parameter in control strategy. For this purpose, the optimal number MR-dampers were determined by DE in section 5. In each time step, the following mechanical model of 20-Ton MR-damper was employed to simulate the control force. The governing equations of MR dampers are described as below:

$$\begin{aligned}
 \dot{y} &= \frac{1}{C_0 + C_1} [\alpha \cdot Z + C_0 \cdot \dot{x} + K_0 (x - y)] \\
 f &= C_1 \cdot \dot{y} + K_1 \cdot (x - x_0) \\
 \dot{Z} &= -\gamma |\dot{x} - \dot{y}| Z |Z|^{n-1} - \beta \cdot (\dot{x} - \dot{y}) |Z|^n + A \cdot (\dot{x} - \dot{y})
 \end{aligned} \tag{3}$$

In the above equations, the parameters described as follows:

$$\begin{aligned}
 \alpha(i) &= 16566 \cdot i^3 - 87071 \cdot i^2 + 168326 \cdot i + 15114 \\
 C_0(i) &= 437097 \cdot i^3 - 1545407 \cdot i^2 + 1641376 \cdot i + 457741 \\
 C_1(i) &= -9363108 \cdot i^3 + 5334183 \cdot i^2 + 48788640 \cdot i - 2791630
 \end{aligned} \tag{4}$$

In the above equation, x and y are the absolute and internal displacement of MR damper, respectively. $\alpha(i)$, $C_0(i)$ and $C_1(i)$ values of MR damper are experimentally determined and 'i' is the input current, in each time interval. Other additional parameters are presumed to be constant as $n=10$, $x_0=0.18$ m, $A=2679$ m⁻¹, $k_1=617.31$ N/m, $k_0=37810$ N/m, γ and $\beta=647.46$ m⁻¹, to validate the experimental data. A first order filter is also utilized to correctly adjust the dynamic mechanical model with experimental data[32]:

$$H(S) = \frac{31.4}{S + 31.4} \tag{5}$$

Where S is the factor to correct the damper rod velocity which is estimated by a Kinematic Kalman Filter (KKF) from the relative displacement between base and first mass and from the absolute acceleration of the first mass [12-14]. The efficacy of time-delay could be eliminated because the time-delay is far from the first period of ordinary structures. The cumulative time-delay associated with the closed-loop control and MR damper was less than 10 milli-second [33]. The electrical inducing current plays the main role to adjust the MR-damper external force during each time-step. The input current is managed by FLC. The governing equations were expresses in the section 5. The configuration of MR damper was illustrated in Fig.1.

3. Fuzzy logic controller

The classical controllers (such as H_2 , LQR, etc.) rely heavily on accuracy of modelling details, uncertainties and nonlinearities in magnitude of the loading and structural properties. The next generation of structural controllers could enhance the uncertainties and imprecisions of modeling without necessitating to solve any optimization prob-

lems. The proposed FLC (Fuzzy Logic Control) includes four elements to resemble the logical-reasoning of human brains. These elements are introduced as defuzzification interface, decision-making, rule base and fuzzification interface. A DE-FLC controller has been proposed to manage the uncertainty and imprecision which was not considered in the controller design process. A closed-loop semi-active feedback controller was generated, based on the following inference rules in Table 1.

Nine linguistic parameters were utilized as output and input fuzzy variables, such as ND (Negative-Displacement), NV (Negative-Velocity), ZD (Zero-Displacement), ZV (Zero-Velocity), PD (Positive-Displacement), PV (Positive-Velocity), L(Large), S(Small) and Z(Zero). To improve the efficiency of input variables in FLC, an independent sensor for each MR damper is defined to transmit the velocity and displacement of sensors. The FLC is governing the MR damper by transmitting inducing current as FLC output variable. In the proposed FLC, range of membership functions for the output and input variables are [0,1] and [-1, 1], respectively. FLC decides no significant control force is required, if the velocity and the displacement of the MR-damper are non-directional. At the other side, a major control force is mandatory, if they are in same direction. In the logical process of determining control output-force, the gaussian curve membership functions were utilized. By utilizing the Mamdani-type fuzzy logic, the transmitted signal of sensors changes into linguistic-fuzzy values. Fig.2 illustrates the membership functions of output and input variables. The scale factor and quantification factor are determined by trial and error to improve the optimal reduction in structural responses.

4. Dolphin echolocation Optimization Algorithm (DE)

The computational time of control system should be minimized to eliminate the time delay effects. The Dolphin Echolocation algorithm demonstrated the fast and reliable optimization in comparison with other algorithms[17-20]. Kaveh and Farhodi introduced a novel optimization algorithm, which was inspired from Dolphin echolocation in nature[21]. The DE did not require extensive computational burden and parameter tuning. It could be widely utilized to solve in various fields of optimization problems. Dolphins are capable to produce signals in the form of clicks with special frequencies. The part of sound-signal energy is reverberated back to the dolphin when the signal collides an object. At the start, Dolphins search all around the search-space to specify the prey. They regenerate sound signals sequentially to estimate the space between the objects by analyzing the time gap between echo and click. Moreover, the direction of object movements can be estimated by compare the strength of the signal from two edges of the dolphin's head. Dolphin reiterates incrementally generating clicks and obtaining echoes in that way until the target has been captured. It could be idealized that echolocation is familiar to optimization in some forms. The procedure of searching preys by employing echolocation in dolphins is similar to concentrating on the optimal location in optimization problems. In DE optimization algorithm, two phases could be defined. At start phase, the DE searches all around the search-space to accomplish a comprehensive search. This procedure is executed by tracking some random locations in the search-space, and in the next phase, DE focuses on exploration around superior obtained results from the prior-step. The metaheuristic values of DE parameters have been proposed by previous researches[34]. The structure of the DE algorithm and the steps involved are illustrated in Figure 3.

Meta-heuristic algorithms characterize better proficiency in sorted design spaces. Therefore, before to beginning the search procedure, the design search space to be sorted out. A curve should be determined, based on the convergence factor during the optimization procedure. The adjustment of CF is expressed as follows:

$$PP(Loop_i) = PP_1 + (1 - PP_1) \frac{Loop_i^{power} - 1}{(LoopsNumber)^{power} - 1} \quad (6)$$

In the above equation, PP , PP_1 , $Loop_i$, $power$ and $Loops Number$ were defined probability, the convergence factor of the start loop, the number of the running loop, the degree of the curve and number of loops in which the algorithm should converge into the optimal point, respectively. The solution of traditional FLC is assumed to be one the solutions to reach the optimal value of MR damper inducing current.

The following procedure of DE algorithm for discrete optimization should be peruse to reach the optimal location:

- 1) Spread NL placements for each dolphin in a random manner. This phase includes generating $L_{NL \times NV}$ matrix. The NV and NL are the number or dimension of each placement and number of dolphin's placement, respectively.
- 2) By using Eq.1, compute the *PP* of the loop.
- 3) Compute the objective of each placement. Fitness functions should be specified in a way, which the better results get higher magnitudes based on Eq.10.
- 4) Compute the accumulative objective function, based on dolphin rules by the following process:
 - 4.a) For $i = 1$ to the number of dolphin's placement
 - For $j = 1$ to the number of dimensions
 - For $k = -R_e$ to R_e

Determine the location of L (i, j) in j-th column of the alternative's matrix as A.

$$AF_{(A+k)j} = \frac{1}{R_e} \times (R_e - |k|) \times Fitness(i) + AF_{(A+k)j} \quad (7)$$

End
End
End

In the above equation, $AF_{(A+k)j}$ was the accumulative objective function of the (A+k)th alternative (numbering of the alternatives is identical to the ordering of the Alternative matrix) to be elected for the j-th variable. Furthermore, R_e was the efficient radius of search area in which accumulative fitness of the alternative A's neighbors were impressed from its fitness values. The search radius is recommended to be less than 1/4 of the search-space. Moreover, $Fitness(i)$ was the fitness value in the placement of i. It should be increased that for alternatives near to sides (where A+k was not a valid; $A+k < 0$ or $A+k > L_{Aj}$), the AF was computed using reflective specifications. Thus, if the distance of an alternative to the side was not more than R_e , it was assumed that the same alternative exists where mentioned alternative could be observed, if a mirror was positioned on the side.

4.b) In order to spread the possibility equal in the search-space, a tiny value was randomly added to all the arrays as $AF = AF + \epsilon$. Based on the way the fitness was determined, ϵ should be determined. It should be less than the minimum value gained for the fitness.

4.c) determine the optimal placement of this loop and name it "The optimum placement". Determine the alternatives assigned to the variables of the optimum location, and let their AF is assumed to be zero.

- 5) For variable j (j=1 to NV), compute the probability of determining alternative i (i=1 to L_{Aj}) as follows:

$$P_{ij} = \frac{AF_{ij}}{\sum_{i=1}^{L_{Aj}} AF_{ij}} \quad (8)$$

- 6) specify a probability equal to *PP* to all alternatives elected for all variables of the optimum placement and devote rest of the probability to the other alternatives as follows:

for $j = 1$ to Number of variables

for $i = 1$ to Number of alternatives

if $i =$ The best location(j) of dolphins

PP = P_{ij}

else

PP = $(1 - PP) \cdot P_{ij}$ (9)

end

end

end

Compute the next phase locations based on the possibilities specified to each alternative. Until Loops Number was received, steps 2-6 have been reiterated. For providing better diversity, the proposed procedure prepares opportunities for the agents to move all over the search-space. The termination criterion was supposed as a maximum number of iterations, which is limited to be 60.

Finally, the population size, N , is specified to be 70. These selections were based on trial and error process to optimize the most appropriate convergence accuracy and speed in the DE algorithm. For each time-window, the fitness function was determined as follows:

$$J_1 = \frac{\sum^n RMS(x_{FLC})}{\sum^n RMS(x_{Poff})} \quad J_2 = \frac{\sum^n RMS(d_{FLC})}{\sum^n RMS(d_{Poff})} \quad J_3 = \frac{\sum^n RMS(\ddot{x}_{FLC})}{\sum^n RMS(\ddot{x}_{Poff})} \quad (10)$$

In the above equation, RMS is the abbreviation of root mean square. Where d , x and \ddot{x} are the inter-story drift, absolute displacement and acceleration of the floors, respectively. The P_{OFF} superscript indicates the case where the dampers were operated in the passive-off mode and MR damper acts as a passive viscous device. The final case was the FLC. In this case, the operational range of each MR damper was determined to be in 0 to 1 V.

5. Numerical simulations and results of DE-FLC

Based on the heavily computational burden, which is required in several seismic time history analyses. In this research, the utilization of ETA analysis is proposed to reduce the time and number of analysis requirement in designing of semi-active controller system. For this purpose, the numerical results are performed in MATLAB software by using the state-space model.

5.1. Optimal sensor and damper Placement by using DE algorithm and FLC controller

In this research, an eleven-story concrete moment frame is utilized to illustrate proficiency of the DE-FLC. The modeling assumptions are as follows:

1. Each floor is assumed to be a rigid diaphragm.
2. The mass of each class is considered as a concentrated mass.
3. The behavior of materials in the linear range.

The structural specifications of concrete moment frame including the mass and stiffness of each floor, is demonstrated in Table 2 and Figure 4. The damping matrix is determined by combining the mass and stiffness of the structural system. The coefficients a_0 , b_0 are obtained for the first and second modes of the structural system and the damping coefficient $\xi_i = \xi_j$ are considered 5% in equation 12.

$$[C] = a_0[M] + b_0[K] \quad (11)$$

$$b_0 = \xi_j \times \frac{2}{\omega_i + \omega_j} \quad a_0 = \xi_i \times \frac{2\omega_i \times \omega_j}{\omega_i + \omega_j} \quad (12)$$

At the first step, to illustrate the efficiency of the proposed DE-FLC in time endurance analysis method, the optimal number and location of damper and their sensors should be determined. For this purpose, three fitness functions were utilized in equations 10. The economic considerations should be utilized to determine the number of dampers, because a greater number of dampers lead to more attenuation in seismic responses of building. Therefore, a penalty function should be utilized to achieve the optimum number of sensors and dampers. The following penalty function (PF) was utilized:

$$PF = (2 \times j_1 + 1 \times j_2 + 0.8 \times j_3) \times (1 + ND \times 0.07) \quad (13)$$

Where J_1 , J_2 , J_3 and ND are three objective functions and number of dampers, respectively. A forward-directivity near-fault El-Centro acceleration was utilized to excite the benchmark structure. The Dolphin Echo-location determines the number and arrangement of the dampers and sensors to minimize the structural responses by utilizing PF, J_1 , J_2 and J_3 . Finally, to optimize optimal placement and number, the structural responses were compared with the passive-off and passive-on cases during time-history analysis. The matrix of DE particles includes the number and the arrangement of the MR dampers and their sensors. The propriety of the DE population moderately enhances with respect to equation.13. To enhance the probability of determining the optimum global solution in meta-heuristic algorithms, five independent DE algorithms were started simultaneously. The local and global best parameters were updated in each 5 iterations between these optimization algorithms.

By utilizing 60 initial particles, DE could determine to the optimal solution after 19th iteration. The optimal solution is determined as follows:

$$\begin{aligned} Dp &= [0 \ 0 \ 2 \ 1 \ 2 \ 2 \ 0 \ 1 \ 2 \ 2 \ 2] \\ Sp &= [- \ - \ 4 \ 6 \ 7 \ 7 \ - \ 8 \ 10 \ 10 \ 11] \end{aligned} \quad (14)$$

Where Dp and Sp are the sensor and damper arrangement vectors, respectively. The DE illustrates that the optimum number of MR dampers is fourteen. Two-200kN MR damper should be placed in the 3rd, 5th, 6th, 9th, 10th and 11th stories and one damper is required in the 4th and 8th stories. Also, their sensors should be placed as shown in Sp vector in the stories of the building. An independent DE-FLC is utilized in each story, which the sensor is installed. Based on the displacement and the velocity transmitted from sensors, DE-FLC decides to transmit the inducing current to generate magnetic field. The viscosity of MR fluid rapidly changes to adjust the required stiffness and damping coefficient in MR damper. Table.3 illustrates the displacement and drift responses of DE-FLC in comparison with other traditional control cases. By utilizing DE-FLC, Significant reductions were obtained in J_1 and J_2 , which correspond to the RMS of the absolute acceleration, inter-story drifts and displacement responses. Based on impact factors were assumed in equations 10, less reduction is obtained in J_3 , which corresponds to the RMS of absolute acceleration in stories. Overallly, the DE-FLC efficiency was superior to passive-on control case with respect to all control cases except the peak absolute acceleration. To indicate the proficiency of DE-FLC more precisely, the controlled responses were compared with passive and semi-active controlled cases. In the passive case, which was indicated by ' P_{OFF} ', no inducing current is transmitted during seismic excitation. In another passive controller which was indicated by ' P_{ON} ', the inducing current was kept constant at the maximum current-inducing value (3.0 A). Furthermore, the proficiency of DE-FLC is compared with previously studied clipped-optimal controller[33].

Results demonstrate that DE-FLC could outstandingly increase the performance of a semi-active controlled structure. The P_{OFF} controller decreases the peak displacement of top-floor by 19% of the uncontrolled responses, the P_{ON} controller demonstrates 32% reduction, the clipped-optimal controller exhibits 29% reduction and the DE-FLC attenuates the responses up to 46%. Despite the reduction of displacement in other controllers, the DE-FLC has demonstrated superior performance in reduction of undesired structural vibration with the same number of dampers and sensors.

5.2. Preparation of Seismic excitation in accordance with ASCE regulations

In this research, ASCE41_06 regulations have been used, which have been presented by ASCE Institute under the title of seismic improvement of buildings[35]. In this regulation, the design of the structure is based on seismic performance, and includes five non-structural performance levels, which are named risk levels. Risk levels include BSE-2 risk level, which represents the most likely earthquake with a probability of occurrence of 2% in 50 years or 2475 years return period and BSE-1 risk level represents 10% probability of earthquake occurrence in 50 years or 475 years return period. Furthermore, two sub-hazard levels, including 20%/50 and 50%/50 years, with 20% and 50% probability of occurrence in 50 years, respectively. According to the rules of this regulation, seven series of accelerometers can be used to analyze the time history and the average response values can be used to evaluate the performance of the structure. In this research, seven earthquake records are selected from the FEMA 440 proposed records for type C soil [36]. After determining the initial coefficients, seven accelerometers should be scaled. The accelerometers should be in the range of 0.2 T and 1.5 T above the spectra of each level of ASCE41 regulations, where T is the period of uncontrolled building. This scale factor was based on the main period of the uncontrolled structure. Table 4 illustrates the specifications of seven selective accelerometers and primary scale coefficients under a set called GM 1 and Table 5 illustrates the scale coefficients for an eleven-story structure with main period time of 0.975 second for different risk levels.

5.3. Endurance time method

In the endurance time (ET) method, the choice of the appropriate type of acceleration time ET functions is essential to obtain the consistency and accuracy of the results. Therefore, to estimate the nonlinear responses of seven time-history analysis for the structure equipped with semi active MR damper controller, the sixth generation of ETA20e01-03 functions has been used. The features of this series of generation of ET functions are good

accuracy in nonlinear analyzes as well as covering long periodic periods[37]. The correct interpretation of the responses of the analysis of durability time and how the time mapping in its functions, fully depend on the seismic motion intensity. In other words, it is sufficient that the spectrum of functions of the acceleration time of the resistance at a given time (target time) corresponds to one of the design spectra or the average spectrum of earthquake records or the spectrum of response due to seismic risk analysis. As shown in Figure 5, to determine the target time series e , it was tried to use the mean spectrum of ASCE41–17 matching of these functions with the mean range of the set (GM1), which is shown in Table 6. By using new approach for ETA method [38-39], time-domain spectral matching algorithm was modified and utilized in several time durations. Furthermore, the matching precision is significantly enhanced, and the computation time is attenuated.

5.4. Evaluation of time endurance curve by using DE-FLC

After the development of the Dolphin Echolocation-Fuzzy Logic Controller (DE-FLC), the performance of proposed controller in reducing structural seismic responses is investigated on the ET curves. The structure is examined by considering the relative displacement of floors as well as the maximum displacement of the last floor in the case before and after the rehabilitation by MR dampers. Figures.6 illustrate the maximum displacement of the top floor under 6th generation ETA20e01, ETA20e-02 and ETA20e-03 accelerations, respectively. The results demonstrate that optimal placement of MR damper by using DE-FLC controller has reduced the maximum displacement of the top floor by 30% to 40%. Figure.7 demonstrates the maximum displacement of the top floor under Morgan Hill, Landers and Northridge seismic excitations, respectively. In this case, the mean of ETAs results can simulate the displacement of top story in the structure under mean of seven real seismic excitations.

To investigate more precisely of risk levels, the results of ETA method are usually provided with the help of an incremental curve. In this curve, the horizontal and vertical axis are the time and maximum drift response of the structure under different demand parameters, respectively. In this research, these curves are also smoothed using the moving average method to eliminate stagnation. In Figure 8, the ETA curve for the structural system is drawn in two case of uncontrolled and DE-FLC controlled. The relative displacement of the floors is illustrated in all cases and then the drift results are compared with the allowable limits of the ASCE regulations. According to the ASCE41-17 regulations, the allowable values of relative displacement of the structural system are considered to be 5% for CP level, 2.5% and 0.7% for LS and IO level, respectively. Therefore, the structure must satisfy the Collapse Prevention at the BSE-2 risk level and the Life Safety level at the BSE-1 risk level [35]. It can be seen from Figure 8, the structure performed poorly without any damper, but the addition of MR dampers with DE-FLC controller could change the performance of the structure in ASCE levels.

By using DE-FLC controller, the endurance time of structure increased from 6.31 (s) to 9.56 (s) in ETA curves. In the other word, the rehabilitated structure could resist against BSE-2 seismic excitation. Figures 9 and 10 demonstrate a comparison between the relative displacement of the floors under the acceleration functions of ETA20e01-03 and GM1 excitation series. It can be observed the relative displacement of the building in general has had a downward trend, and the same results are observed in the study of ETA functions without necessitating heavily nonlinear complex time history analysis. Thus, it can be said that the mean of ETA functions has provided a good prediction of the behavior of the structure under mean of several earthquake records.

The relative displacement of the floors in cases of uncontrolled and controlled with DE_FLC for the BSE-2, BSE-1 and 50%/50 years hazard levels has been investigated in Figures 11 and 12. To evaluate the performance of the DE-FLC in reduction of the seismic response of the structure, the ETA curves have been compared with seven GMI records. As can be seen, the structure had seismic responses close to the limits of the ASCE regulations and even beyond before the rehabilitation with DE-FLC. The DE-FLC could efficiently improve the seismic performance of the structure to the allowable ASCE drift ratio by decreasing the responses. At the BSE-1 hazard level, the drift ratio of the building is reduced by 24%, indicating the proper efficiency of DE-FLC. Fur-

thermore, it can be seen that the ETA curve could predict the trend of displacement as same as structural responses of the average of seven GM1 series records.

It can be seen from the results that the ETA curves could predict the different level of structural seismic demands. Table. 7 demonstrate the precision of ETA curves in comparison with seven seismic excitations of GMI records.

It could be summarized generally; the simulation results demonstrate that sixth generation of ETAs can simulate the vibration results of time history analyzes well without necessitating any heavily constrained computational burden. The mean of error percentages for drift ratio in case of ETA analysis are 8%, 8% and 7% for uncontrolled cases and 12%, 8% and 8% for controlled cases, in different seismic risk levels respectively. The error percentages of ETA analysis in comparison with the mean of several time history analysis were less than 15% under BSE-1 and BSE-2 seismic risk levels. In comparison with risk level of 50% in 50 years, the error in worst case, reached to 17.4% but the mean of errors in all stories was acceptable.

6. Conclusions

A novel Dolphin Echolocation was utilized to optimize the sensor and MR damper arrangement for the attenuation of building responses subjected to GMI series and 6th generation of ETA records. Furthermore, DE-FLC Controller was introduced to administrate inducing-current of the MR-dampers in semi-active controlled structure. Numerical results and simulation were accomplished to illustrate the proficiency of Dolphin Echolocation-Fuzzy Logic Controller (DE-FLC). The DE_FLC can reduce the structural responses up to 30-40% in comparison with uncontrolled case. The simulation efforts demonstrate that modified DE-FLC controller is a practicable technique and superior from clipped optimal control.

Moreover, numerical studies have been done to demonstrate the ability of sixth generation of ETA to simulate the responses of controlled structure as well as time history analyzes without necessitating any heavily constrained computational burden. The following result can be summarized:

1. The DE_FLC can attenuate the maximum displacement of the top floor and drift about 30% and 40%. It also reduces the relative displacement between the floors and the maximum allowable limits set in the ASCE regulations are observed.
- 2 - The target time of ETA curves increases from 6.31 seconds to 9.31 by using DE-FLC controller, which indicates the increase in structural durability time.
- 3- The results demonstrate that durability method has the ability to predict the behavior of semi-active controlled structures with a minimum number of analyzes with appropriate error percentage. The ETA can predict the drift trend in stories and risk levels with a reasonable approximate.
- 4 - Comparing the trend of changes in structural response diagrams under series E of ETA and seven selected GMI accelerometers, it can be concluded that the responses resulting from the ETA provide an acceptable estimate of the actual acceleration responses and have a maximum error of less than 18%.

Biographies

Farzam MoghadamRad received his bachelor of civil engineering degree from Tehran University in 2002. His earthquake engineering master from Science and Research Branch of Islamic Azad University in 2005 and he is PhD candidate in that university. He is a teacher at Parand Branch of Islamic Azad University and Engineering system organization. His areas of research include masonry and concrete structure design and execution, wavelet analyses and active and semi-active control.

Panam Zarfam received his PhD of structure engineering degree from Sharif University. He is a Professor at the Civil Engineering Department at Department of Structural Engineering, Science and Research Branch of Islamic Azad University where he taught several graduate and undergraduate courses, supervised many PhDs, and master students. His areas of research include structure design, nonlinear analysis, seismic design and active and semi-active control.

Masoud Zabihi-Samani is an assistant professor in the field of structural engineering. He received his PhD degree from Iran University of science and technology in 2014. He is a Professor and Faculty of civil engineering department at Parand Branch of Islamic Azad University where he taught several graduate and undergraduate courses, supervised 4 PhD and more than 40 master students. Professor ZabihiSamani's area of research includes vibration control of structural systems, time endurance method, active & semi-active control, system identification, wavelet & curvelet analysis and corrosion in concrete structures, in which he has published more than 60 peer-reviewed journal and conference papers nationally and internationally.

7. REFERENCES

1. Aghajanian, S., Baghi, H., Amini, F. *et al.* "Optimal control of steel structures by improved particle swarm", *International Journal of Steel Structures*, **14**(2), p. 223-230 (2014).
2. Amezcua-Sanchez, J. P., Valtierra-Rodriguez, M., Aldwaik, M., et al., "Neurocomputing in Civil Infrastructure". *Scientia Iranica*, **23**(6), p. 2417-2428 (2014).
3. Fisco, N.R. and H. Adeli, "Smart structures: Part I—Active and semi-active control", *Scientia Iranica*, **18**(3), p. 275-284 (2011).
4. Zabihi-Samani, M. and F. Amini, "A cuckoo search controller for seismic control of a benchmark tall building", *Journal of Vibroengineering*, **17**(3): p. 1382- 1400 (2015).
5. Zabihi-Samani, M. and M. Ghanoooni-Bagha, "Optimal Semi-active Structural Control with a Wavelet-Based Cuckoo-Search Fuzzy Logic Controller", *Iranian Journal of Science and Technology, Transactions of Civil Engineering*, pp. 619–634 (2018).
6. Bigonah, M., Soltani, H., Zabihi-Samani, M., et al. "Performance evaluation on effects of all types of infill against the progressive collapse of reinforced concrete frames", *Asian Journal of Civil Engineering*, **21**(3): pp. 395-409 (2020).
7. Honarvar, H., Shayanfar, M.A., Babakhani, B., et al. "Numerical Analysis of Steel-Concrete Composite Beam with Blind Bolt under Simultaneous Flexural and Torsional Loading", *Civil Engineering Infrastructures Journal*, **53**(2): pp. 379-393 (2020).
8. Sodeyama, H., K. Suzuki, and K. Sunakoda, "Development of Large Capacity Semi-Active Seismic Damper Using Magneto-Rheological Fluid". *Journal of Pressure Vessel Technology*, **126**(1): pp. 105-109 (2004).
9. Spencer, B.F., Dyke, S. J., Sain, M. K., et al. "Phenomenological Model for Magnetorheological Dampers", *Journal of Engineering Mechanics*, **123**(3): pp. 230-238 (1997).
10. Azimi, M, Rasoulnia, A, Lin, et al. "Improved semi- active control algorithm for hydraulic damper- based braced buildings". *Structural Control and Health Monitoring*, **24**(11): pp. e1991 (2017).
11. Zabihi-Samani, M. "Design of Optimal Slit Steel Damper Under Cyclic Loading for Special Moment Frame by Cuckoo Search". *International Journal of Steel Structures*, **19**(4): pp. 1260-1271 (2019).
12. Vaishnav, S., J. Paul, and R. Deivanathan "Model development and simulation of vehicle suspension system with magneto-rheological damper". *IOP Conference Series: Earth and Environmental Science*, **850**(1): p. 012035 (2021).
13. Li, G. and Z.-B. Yang "Modelling and Analysis of a Magnetorheological Damper with Nonmagnetized Passages in Piston and Minor Losses". *Shock and Vibration*, **2020**, pp. 20521-40 (2020).
14. Zhang, S., W. Shi, and Z. Chen "Modeling and Parameter Identification of MR Damper considering Excitation Characteristics and Current". *Shock and Vibration*, **2021**: p. 6691650 (2021).
15. Sabbagh-Yazdi, S.R., Farhoud, A. & Zabihi-Samani M. "Transient Galerkin finite volume solution of dynamic stress intensity factors". *Asian Journal of Civil Engineering*, **20**(3): pp. 371-381 (2019).
16. Thomas, J., C. Moss, and A. Vater "Echolocation in Bats and Dolphins", *Bibliovault OAI Repository*, the University of Chicago Press, (2007).
17. Saedi Daryan, A., Salari, M., Farhoudi, N. et al. "Seismic Design Optimization of Steel Frames with Steel Shear Wall System Using Modified Dolphin Algorithm", *International Journal of Steel Structures*, **21** (2021).
18. Dehghani, M., M. Mashayekhi, and M. Sharifi "An efficient imperialist competitive algorithm with likelihood assimilation for topology, shape and sizing optimization of truss structures", *Applied mathematical modelling*, **93**: p. 1-27 (2021).
19. Palizi, S. and A. Saedi Daryan "Plastic Analysis of Braced Frames by Application of Metaheuristic Optimization Algorithms", *International Journal of Steel Structures*, **20**(4): pp. 1135-1150 (2020).
20. Wei, C., Hoffmann-Kuhnt, M., Au, W.W.L. et al. "Possible limitations of dolphin echolocation: a simulation study based on a cross-modal matching experiment", *Sci Rep*, **11**(1): pp. 66-89 (2021).
21. Kaveh, A. and N. Farhoudi "A new optimization method: Dolphin echolocation", *Advances in Engineering Software*, **59**: pp. 53-70 (2013).
22. Basu, B. and S. Nagarajaiah "A wavelet-based time-varying adaptive LQR algorithm for structural control", *Engineering Structures*, **30**(9): pp. 2470-2477 (2008).
23. Soto, M.G. and H. Adeli, "Placement of control devices for passive, semi-active, and active vibration control of structures", *Scientia Iranica*, **20**(6): pp. 1567-1578 (2013).

24. G. Yang, B.F. Spencer, J.D. Carlson, et al. "Large-scale MR fluid dampers: modeling and dynamic performance considerations", *Engineering Structures*, **24**(3): pp. 309-323 (2002).
25. Nomura, Y., H. Furuta, and M. Hirokane, "An Integrated Fuzzy Control System for Structural Vibration", *Computer-Aided Civil and Infrastructure Engineering*, **22**(4): pp. 306-316 (2007).
26. MohsenAli Shayanfar, M.B., Danial Sobhani and Masoud Zabihi-Samani "The Effectiveness Investigation of New Retrofitting Techniques for RC Frame against Progressive Collapse", *Civil Engineering Journal*, **4**(9): pp. 2132-2142 (2018).
27. Ostadali-Makhmalbaf, M., M. Tutunchian, and M. Zabihi-Samani "Optimized fuzzy logic controller for semi-active control of buildings using particle swarm optimization", *Advanced Material Research*, **2505**(9): pp. 255-260 (2011).
28. Raji, F. and A. Naeiji "Performance of Concrete MRF at Near-Field Earthquakes Compared to Far-Field Earthquakes", *Civil engineering journal*, **5**(4), pp. 759-766 (2019).
29. Estekanchi, H., Mashayekhi, M., Vafai, H., et al. "A state-of-knowledge review on the Endurance Time Method", *Structures*, **27**(9), pp. 2288-2299 (2020).
30. Rezaei, M., A. Ranjbar Karkanaki, and M. Zabihi - Samani "Experimental Investigation of Deep Beams Containing High-Performance Fiber-Reinforced Cementitious Composite", *Iranian Journal of Science and Technology, Transactions of Civil Engineering*, **46**(1), p. 55-65 (2022).
31. Shirkhani, A. Mualla, I., Shabakhty, N. et al. "Behavior of steel frames with rotational friction dampers by endurance time method", *Journal of Constructional Steel Research*, **107**(5), pp.211-222 (2015).
32. Aggumus, H. and S. Cetin "Experimental investigation of semiactive robust control for structures with magnetorheological dampers", *Journal of Low Frequency Noise, Vibration and Active Control*, **37**(2): pp. 216-234 (2018).
33. Xue, X., Sun, Q. , Zhang, L., et al. "Semi-active Control Strategy using Genetic Algorithm for Seismically Excited Structure Combined with MR Damper", *Journal of Intelligent Material Systems and Structures*, **22**(3): pp. 291-302 (2011).
34. Gholizadeh, S. and H. Poorhoseini "Seismic layout optimization of steel braced frames by an improved dolphin echolocation algorithm", *Structural and Multidisciplinary Optimization*, **54**(4): pp.1011-1029 (2016).
35. "Seismic Evaluation and Retrofit of Existing Buildings", *Seismic Evaluation and Retrofit of Existing Buildings*, ASCE/SEI 41-13 (2014).
36. Khoshnoudian, F. and I. Behmanesh "Evaluation of FEMA-440 for including soil-structure interaction", *Earthquake Engineering and Engineering Vibration*, **9**(3): pp. 397-408 (2010).
37. Sarcheshmehpour, M., H.E. Estekanchi, and M.A. Ghannad "Optimum placement of supplementary viscous dampers for seismic rehabilitation of steel frames considering soil-structure interaction", *The Structural Design of Tall and Special Buildings*, **29**(1): pp. e1682 (2020).
38. Zhang, R., Zhang, L., Pan, C., et al. "Generating high spectral consistent endurance time excitations by a modified time-domain spectral matching method", *Soil Dynamics and Earthquake Engineering*, **145**(5) pp. 106708 (2021).
39. Shayanfar, M., Hatami, A., Zabihi-Samani, M., et al. "Simulation of the force-displacement behavior of reinforced concrete beams under different degrees and locations of corrosion", *Scientia Iranica*, **29**(3): pp. 964-972 (2022).

List of Figures:

Figure.1. MR-Damper Mechanical model [12]

Figure. 2. The input and output membership functions for the proposed FLC

Figure 3: The structure of Dolphin Echolocation algorithm

Figure 4: 11th story benchmark building with possible MR damper location

Figure 5: Rules Spectrum, Scale Measurement Scale (GM1) and e-Series Levels at Different Risk Levels

Figure 6: Displacement of top story in case of uncontrolled and DE-FLC controlled under ETA20e02 and ETA20e03

Figure 7: Displacement of top story in case of uncontrolled and controlled with DE-FLC controlled under the Morgan Hill, Landers and Northridge record

Figure 8: Time Endurance curves of structures in case of uncontrolled and controlled with DE-FLC

Figure 9: Inter-story drift ratio under GMI seismic records

Figure 10. Inter-story drift ratio under ETA records

Figure 11- Inter-story drift ratio under mean of ETA and GMI records in case of uncontrolled

Figure 12- Inter-story drift ratio under mean of ETA and GMI records in case of onttrolled

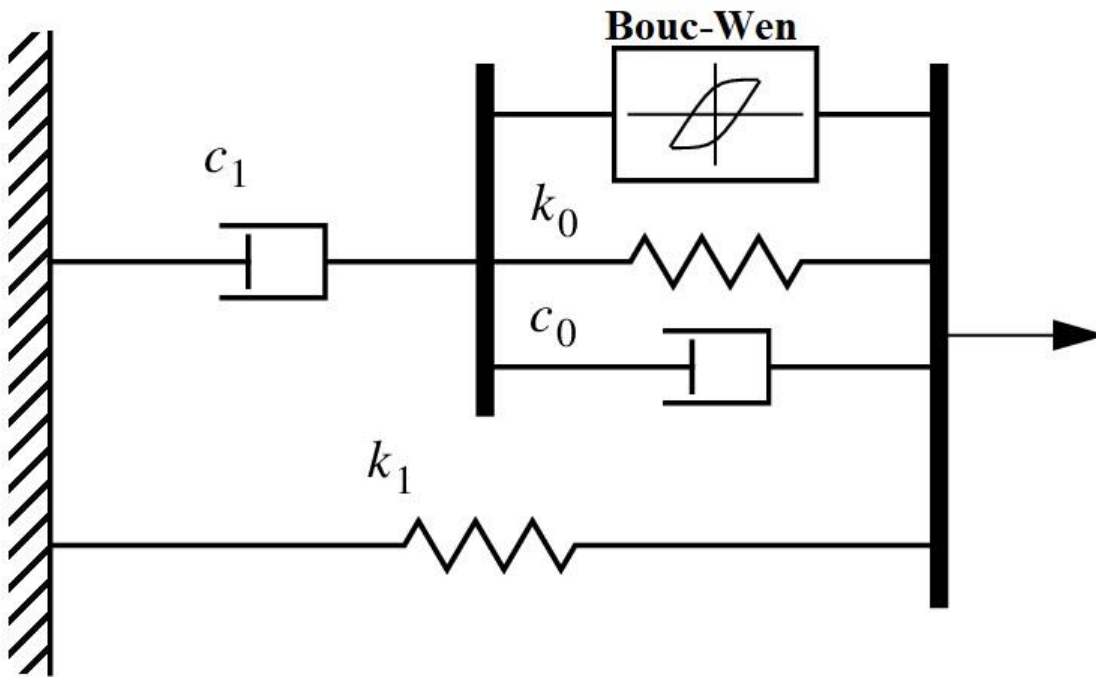


Fig.1. MR-Damper Mechanical model [12]

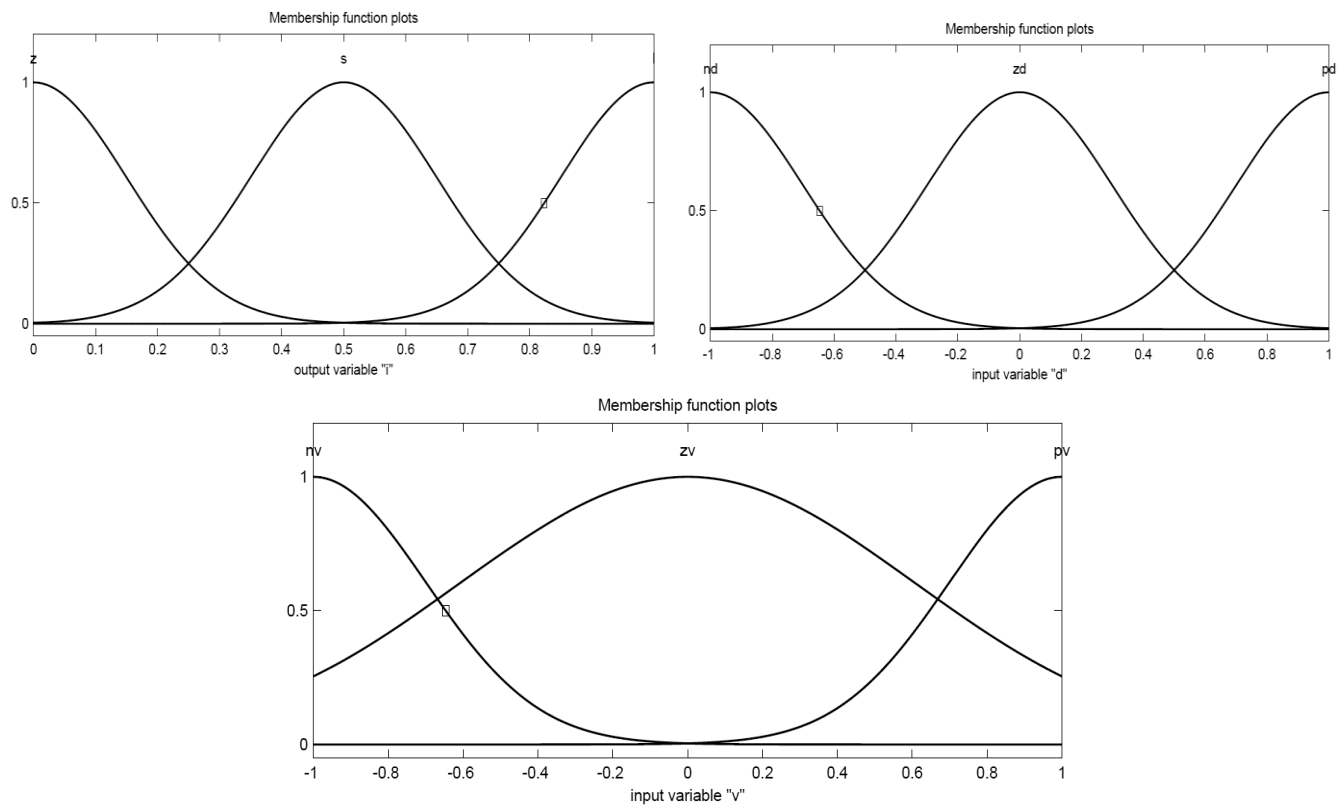


Fig. 2. The input and output membership functions for the proposed FLC

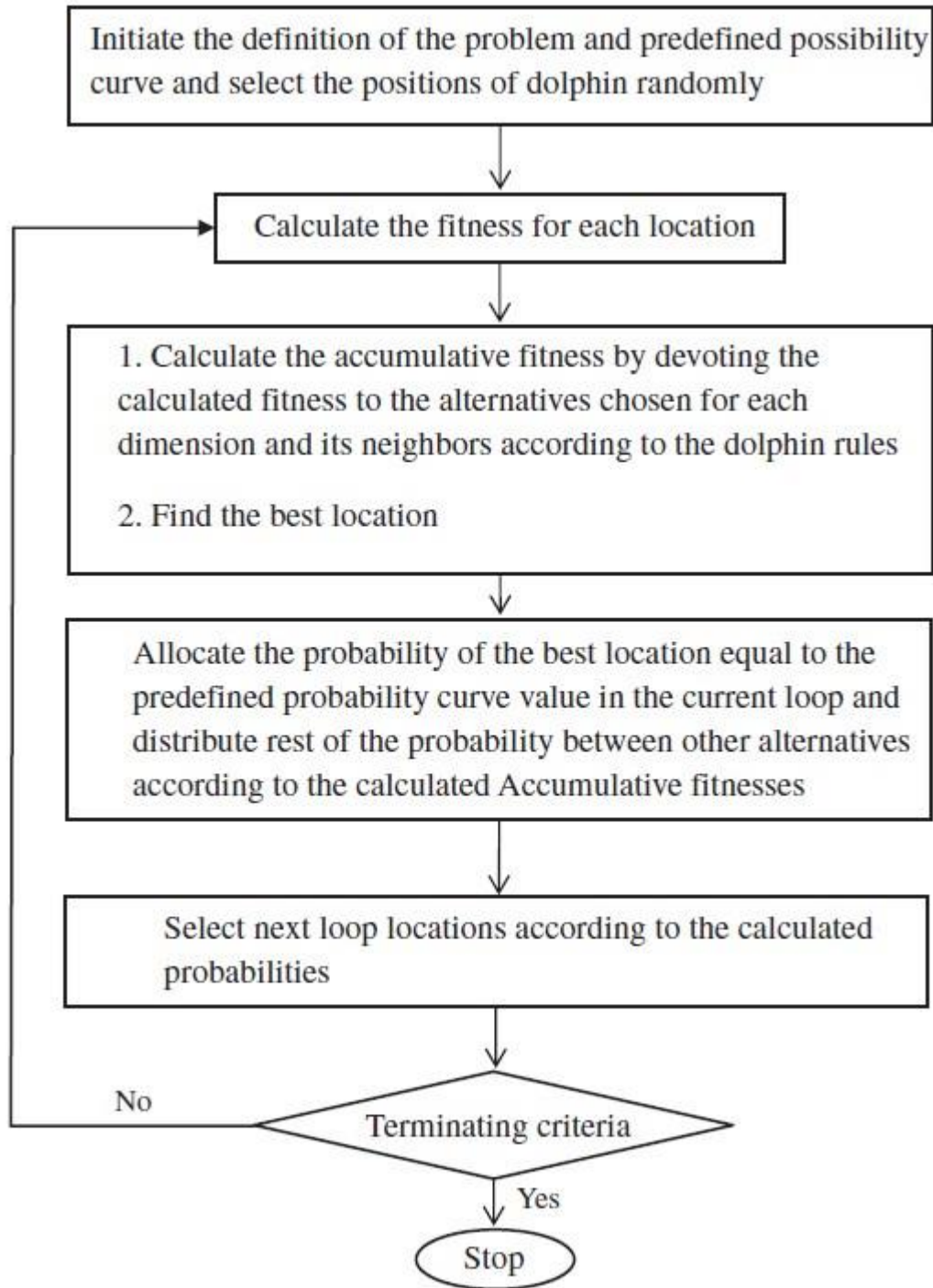


Fig.3. The structure of Dolphin Echolocation algorithm

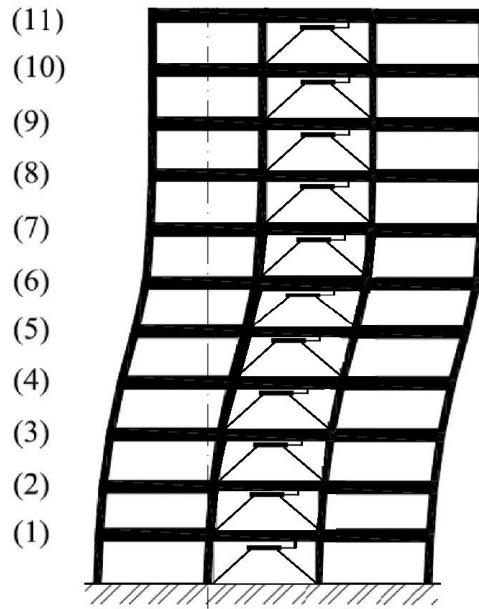


Fig.4. 11th story benchmark building with possible MR damper location

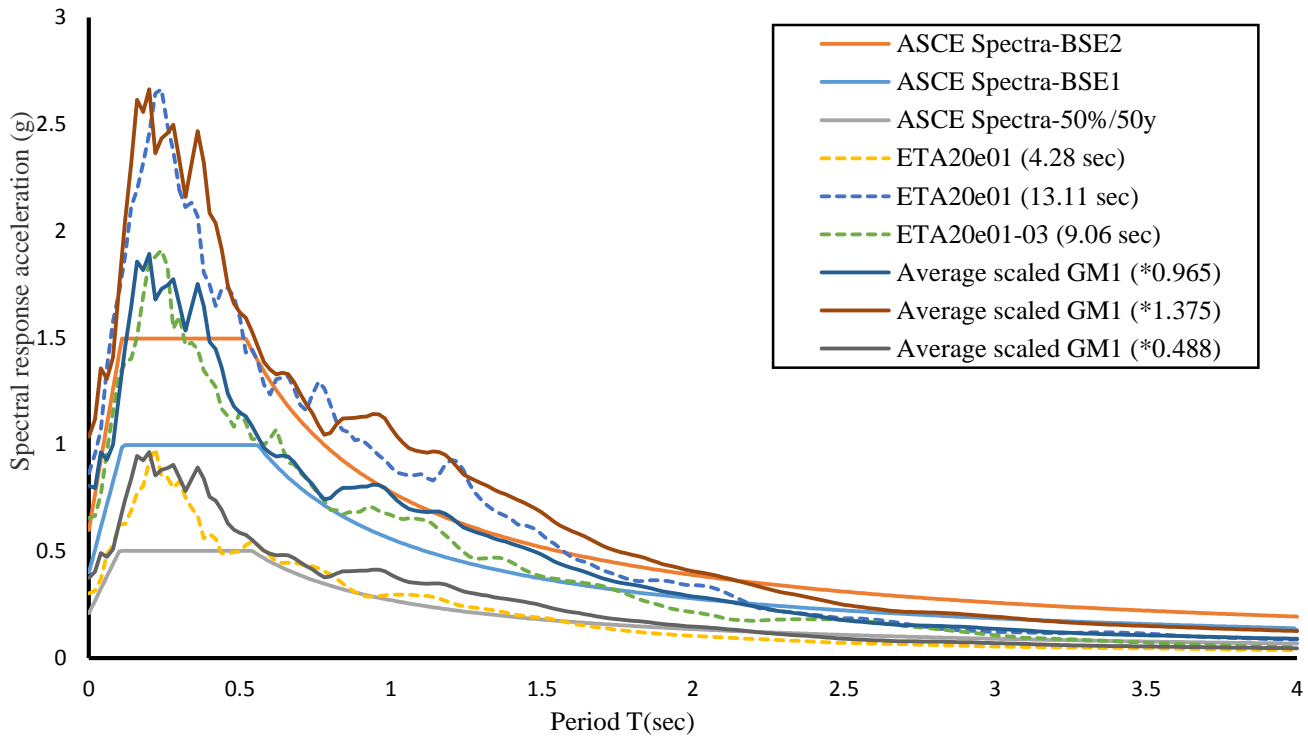


Fig.5. Rules Spectrum, Scale Measurement Scale (GM1) and e-Series Levels at Different Risk Levels

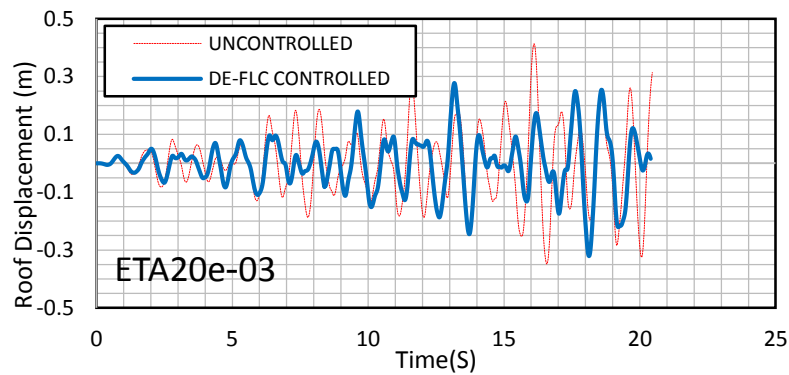
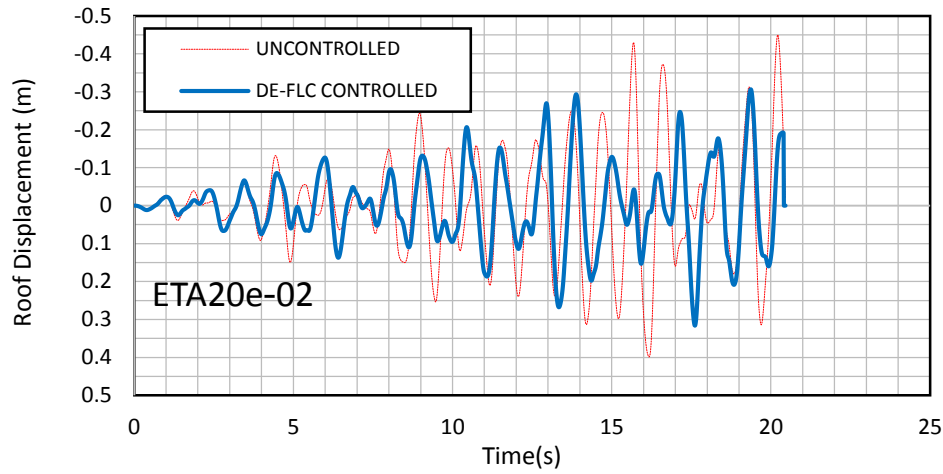
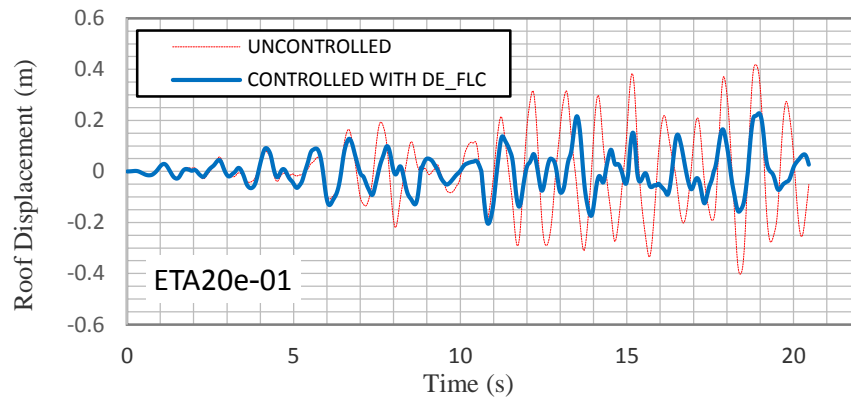


Fig.6. Displacement of top story in case of uncontrolled and DE-FLC controlled under ETA20e02 and ETA20e03

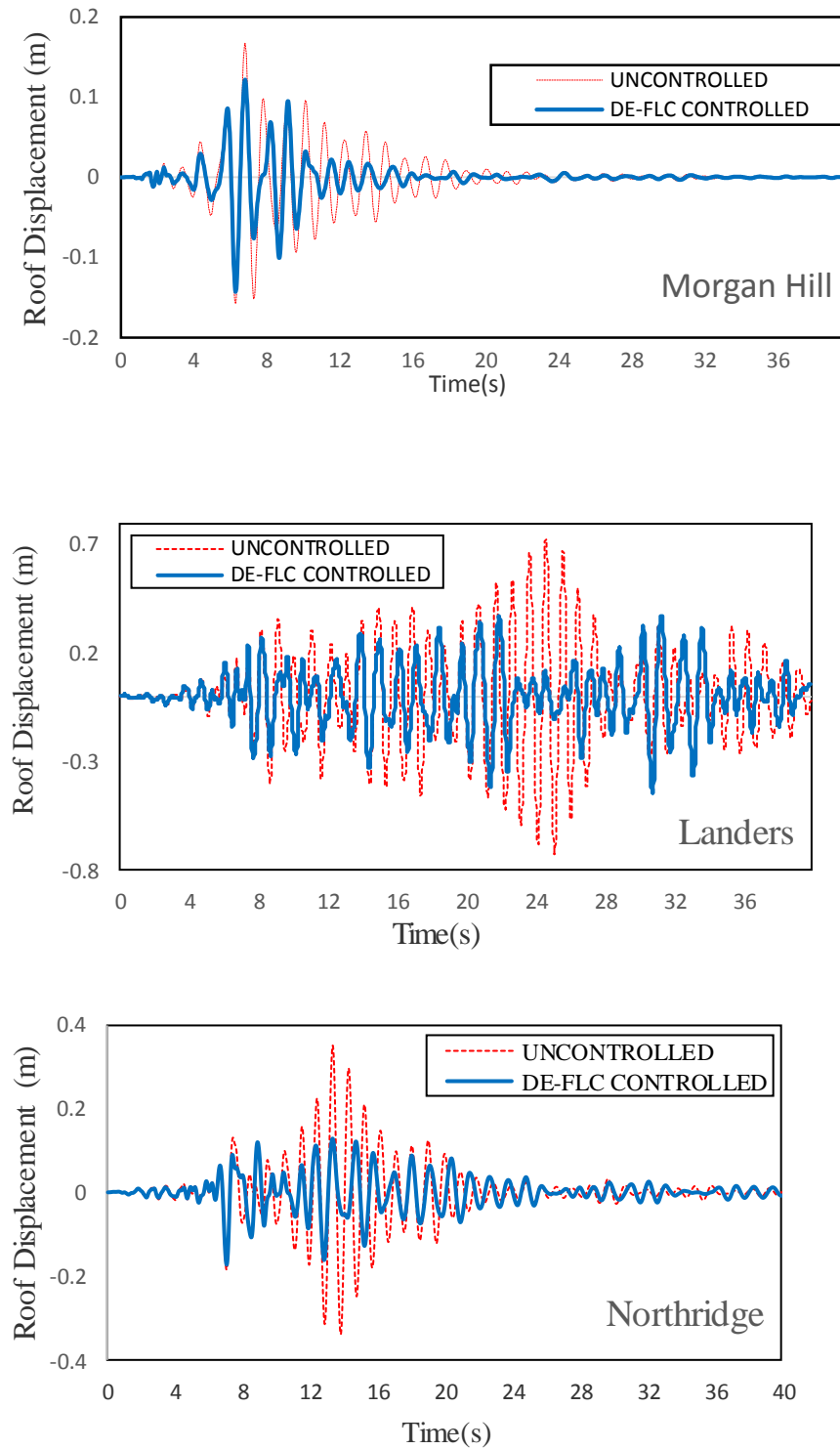


Fig.7. Displacement of top story in case of uncontrolled and controlled with DE-FLC controlled under the Morgan Hill, Landers and Northridge record

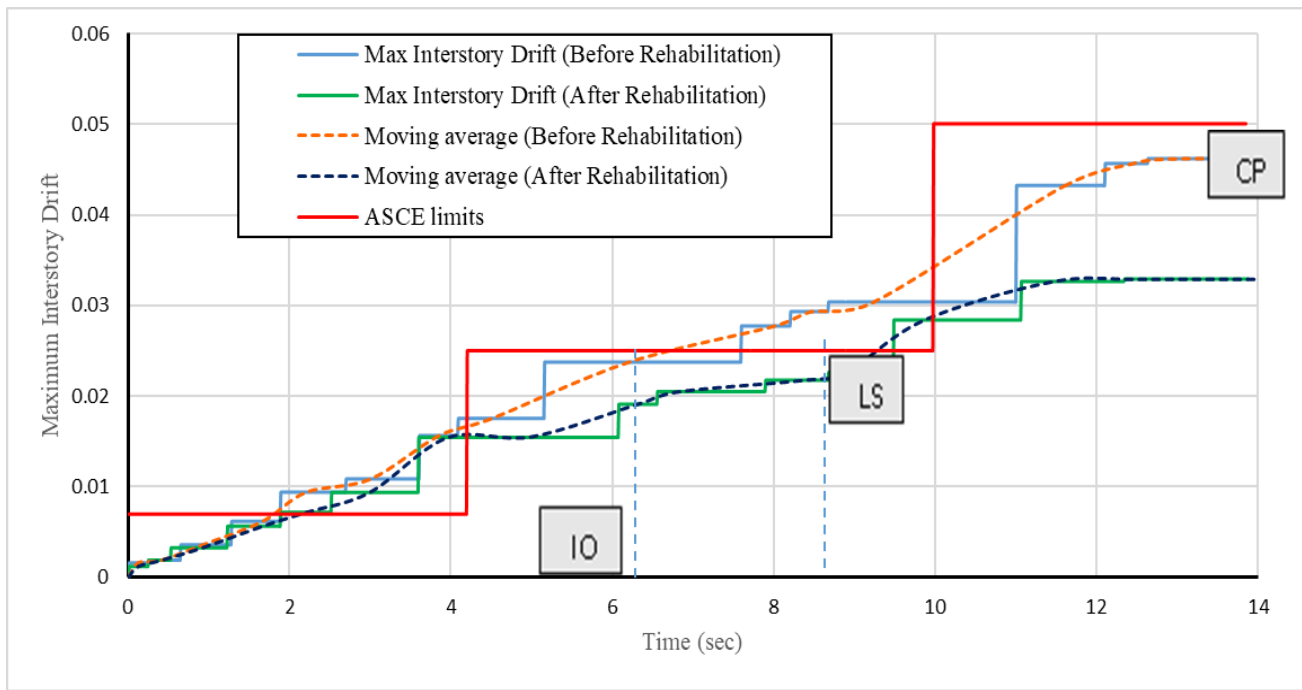


Fig.8. Time Endurance curves of structures in case of uncontrolled and controlled with DE-FLC

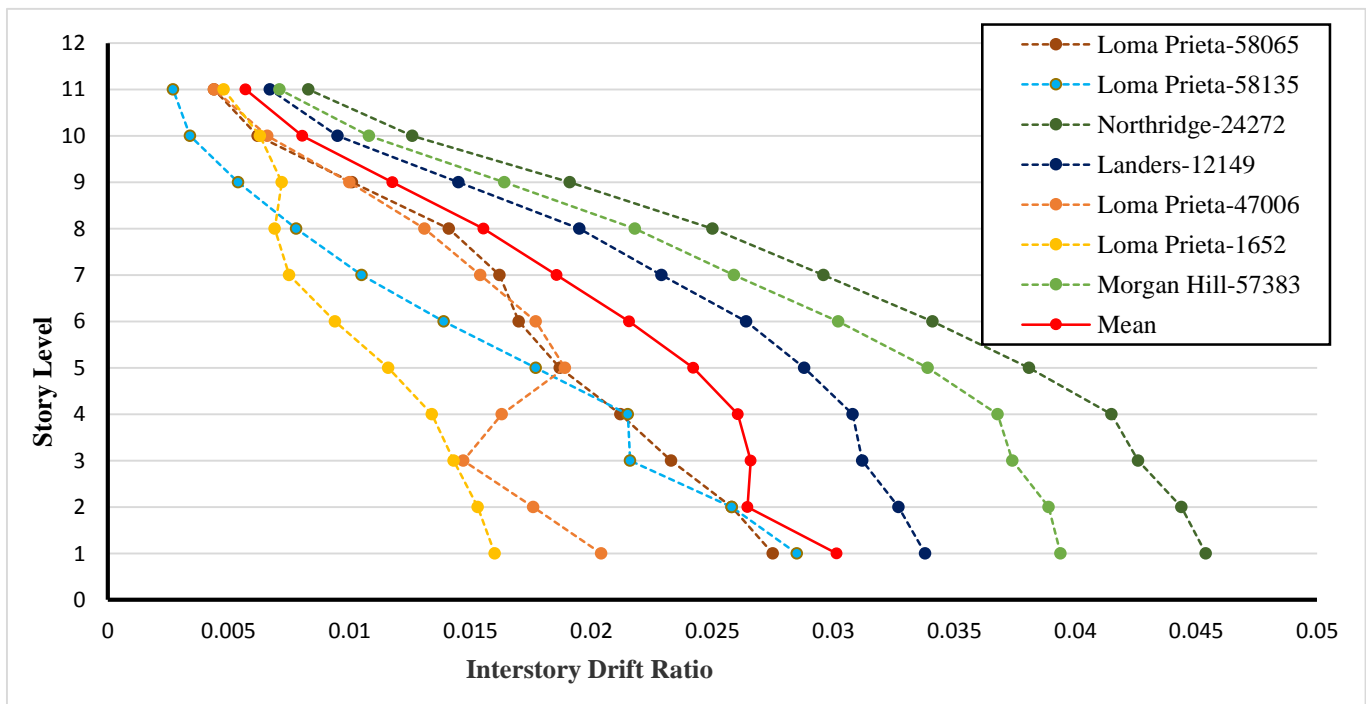


Fig.9. Inter-story drift ratio under GMI seismic records

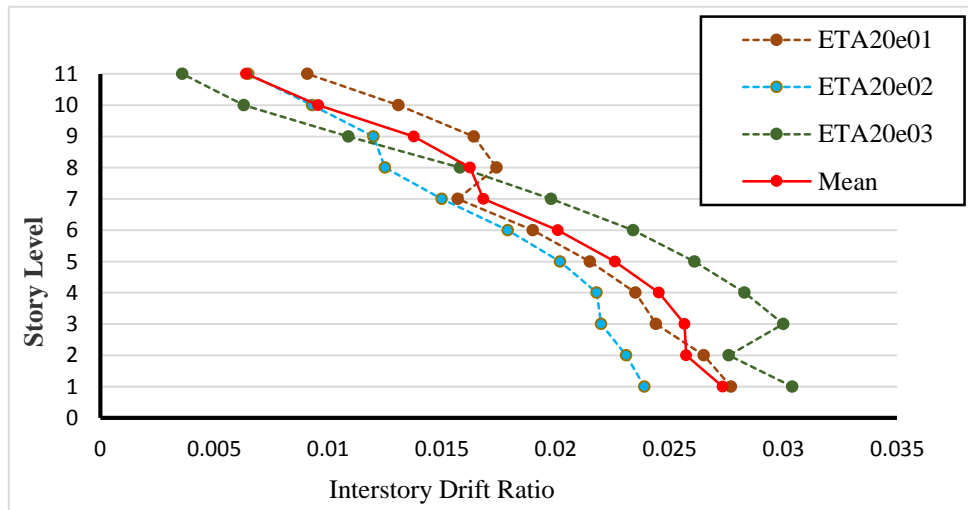


Fig.10. Inter-story drift ratio under ETA records

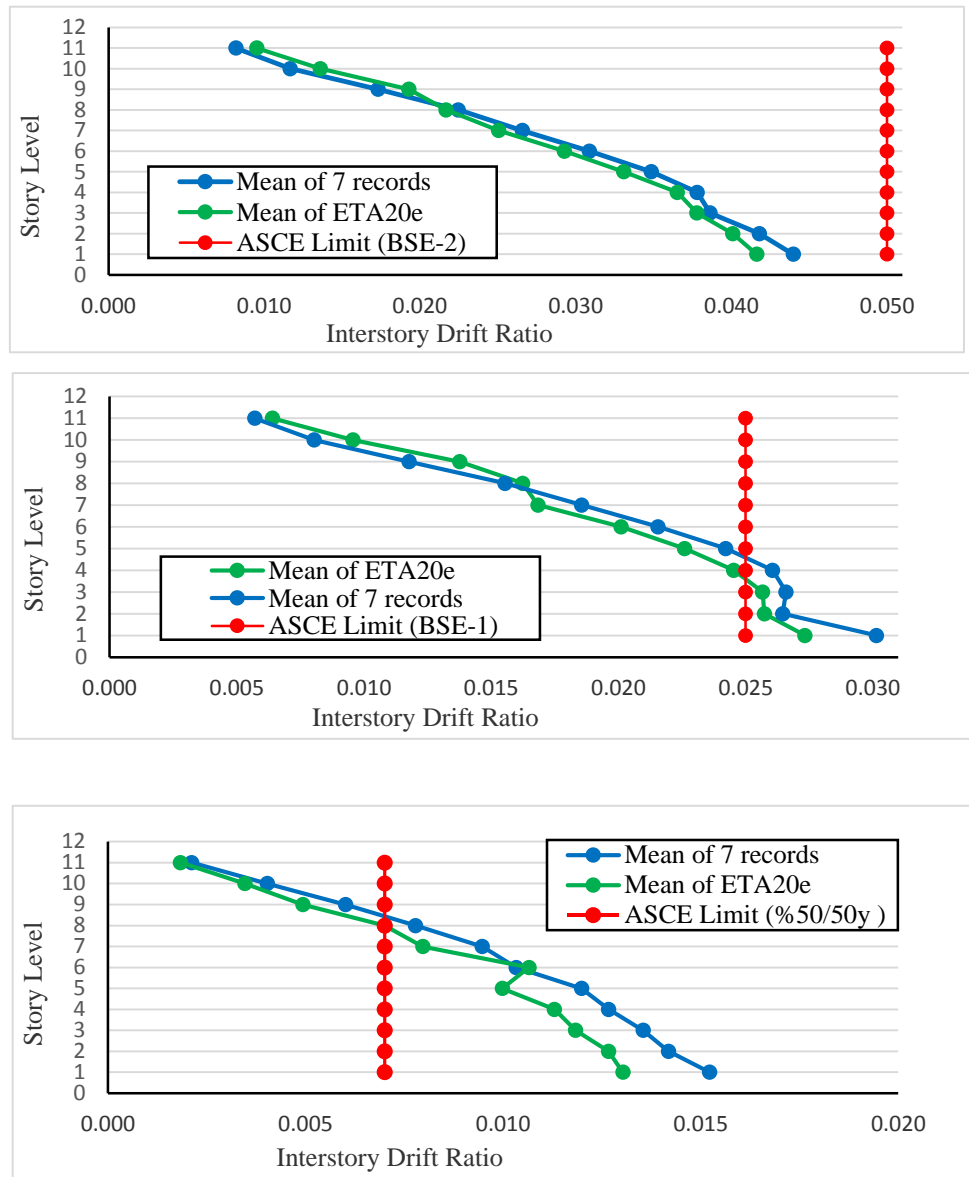


Fig.11. Inter-story drift ratio under mean of ETA and GMI records in case of uncontrolled

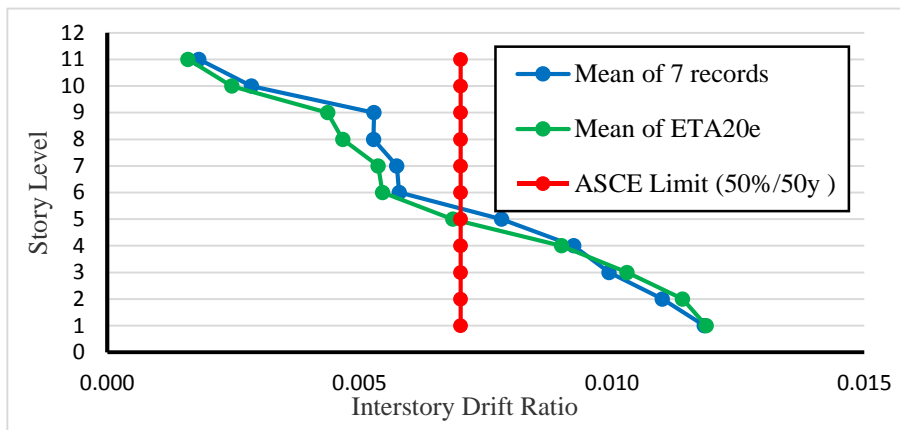
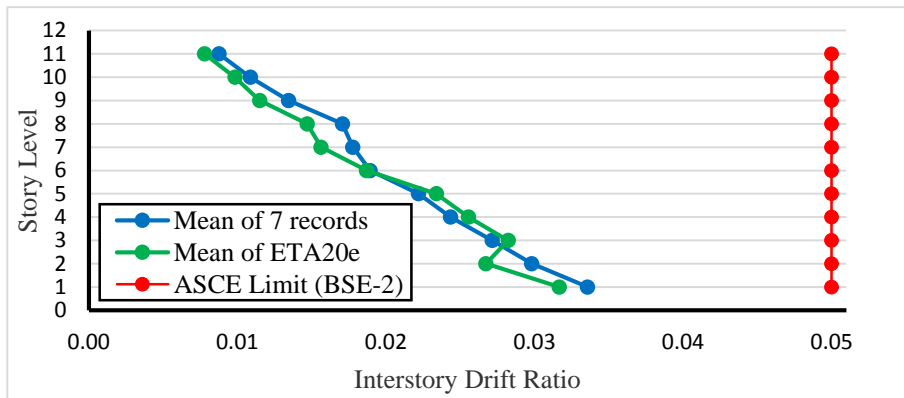
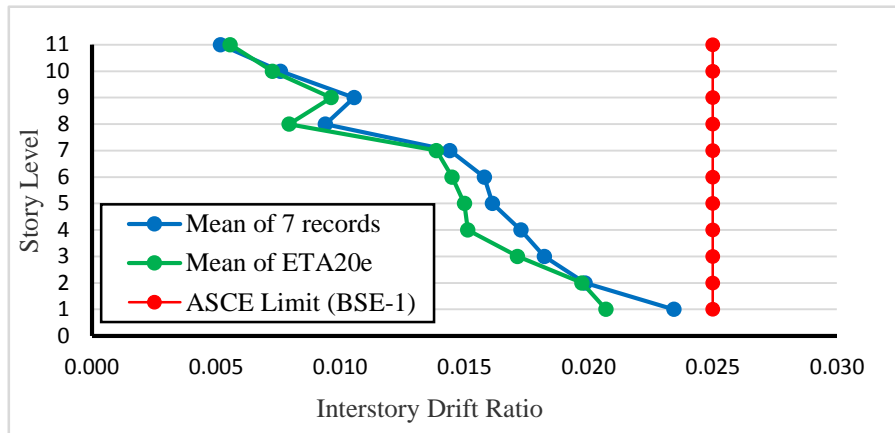


Fig.12. Inter-story drift ratio under mean of ETA and GMI records in case of controlled

List of Tables:

Table 1. The components of suggested FLC

Table 2. The mass and stiffness of concrete moment frame

Table 3. The absolute maximum results of 11th-story structural system[33] in Elcentro earthquake

Table.4. Specifications of seven selective accelerometers based on FEMA-440

Table.5 Scale factor of building based on ASCE41–06

Table 6. Target time function of acceleration time function at ASCE41–17 risk levels

Table 7. Error percentages of drift ratio in case of ETA analysis in comparison with time history analysis

Table 1. The components of suggested FLC

	NV	ZV	PV
ND	L	S	Z
ZD	S	Z	S
PD	Z	S	L

Table 2. The mass and stiffness of concrete moment frame

Number of Stories	Mass (Ton)	Stiffness(kN/m)
1	215	4680
2	201	4760
3	201	4680
4	200	4500
5	201	4500
6	201	4500
7	201	4500
8	203	4370
9	203	4370
10	203	4370
11	176	3120

Table 3. The absolute maximum results of 11th-story structural system[33] in Elcentro earthquake

The Case of Structural responses	Uncontrolled Structure	Controlled Structure			
		P-OFF	P-ON	Clipped-Optimal Controller	DE-FLC
11th floor max drift (cm)	0.114	0.092	0.078	0.081	0.061
11th floor maximum displacement (cm)	0.41	0.33	0.28	0.29	0.24

Table.4. Specifications of seven selective accelerometers based on FEMA-440

Date of occurrence	Station of Earthquakes	Magnitude (Ms)	Station number	Component (deg)	PGA (cm/s ²)	Scale factor
6/28/1992	Landers	7.5	12149	0	167/5	3.64
10/17/1989	Loma Prieta	7.1	58065	0	494/5	1.44
1/17/1994	Northridge	6.8	24278	360	504/2	1.07
4/24/1984	Morgan Hill	6.1	57383	90	280/4	1.84
10/17/1989	Loma Prieta	7.1	47006	67	349/1	2.20
10/17/1989	Loma Prieta	7.1	58135	360	433/1	2.29
10/17/1989	Loma Prieta	7.1	1652	270	239/4	2.61

Table.5 Scale factor of building based on ASCE41–06

Risk Level	Scale factor
BSE-1	0.965
BSE-2	1.375
50%/50year	0.488

Table 6. Target time function of acceleration time function at ASCE41–17 risk levels

Risk levels of ASCE41–17	Mean Target time (S) of ETA20e01-03
BSE-2	13.11
BSE-1	9.06
50%/50 year	4.28

Table 7. Error percentages of drift ratio in case of ETA analysis in comparison with time history analysis

Seismic Risk Level	BSE-2		BSE-1		50%/50 years	
Story	Simulation Error percentage (%)					
	Uncontrolled	DE-FLC Controlled	Uncontrolled	DE-FLC Controlled	Uncontrolled	DE-FLC Controlled
1	0.3	13.4	9.3	11.6	5.35	5.6
2	3.5	10.7	2.7	0.6	4.1	10.3
3	3.5	12.6	3.5	5.9	2.1	3.8
4	2.6	10.8	5.8	12.4	3.3	4.7
5	12.4	14.7	6.7	7	5.1	5.1
6	5.7	3	6.8	8.2	5.2	1.3
7	6.5	13.9	9.3	3.8	5.7	12
8	11.6	10.1	4.3	14.3	3.5	13.8
9	17.4	18	14.1	8.8	10.2	14.4
10	13.7	13.9	14.7	4.2	14.1	9.6
11	11.7	13.3	10.9	7.1	14	11.1